

TITLE PAGE**FULL TITLE: Allele-specific knockdown of mutant HTT protein
via editing at coding region SNP heterozygosities**

AUTHORS: Sarah R. Oikemus¹, Edith L. Pfister², Ellen Sapp³, Kathryn O. Chase², Lori A. Kennington², Edward Hudgens¹, Rachael Miller², Lihua Julie Zhu¹, Akanksh Chaudhary¹, Eric O. Mick⁴, Miguel Sena-Esteves⁵, Scot A. Wolfe^{1, 6}, Marian DiFiglia³, Neil Aronin^{2, 7, 8}, Michael H. Brodsky^{1, 8}

¹Department of Molecular Cell and Cancer Biology, University of Massachusetts Medical School, Worcester, MA

²Department of Medicine, University of Massachusetts Medical School, Worcester, MA

³Department of Neurology, Harvard Medical School and MassGeneral Institute for Neurodegenerative Disease, Charlestown, MA

⁴Department of Population and Quantitative Health Sciences, University of Massachusetts Medical School, Worcester, MA

⁵Horae Gene Therapy Center, University of Massachusetts Medical School, Worcester, MA

⁶Department of Biochemistry and Molecular Pharmacology, University of Massachusetts Medical School, Worcester, MA

⁷RNA Therapeutics Institute, University of Massachusetts Medical School, Worcester, MA

⁸Corresponding Authors

RUNNING TITLE: Gene Editing at HTT Protein Coding SNPs

KEYWORDS: Huntington's Disease, Gene Editing, Single Nucleotide Polymorphism

ABSTRACT

Huntington's disease (HD) is a devastating, autosomal dominant neurodegenerative disease caused by a trinucleotide repeat expansion in the HTT gene. Inactivation of the mutant allele by CRISPR-Cas9 based gene editing offers a possible therapeutic approach for this disease, but permanent disruption of normal HTT function might compromise adult neuronal function. Here, we use a novel HD mouse model to examine allele-specific editing of mutant HTT (mHTT), with a BAC97 transgene expressing mHTT and a YAC18 transgene expressing normal HTT. We achieve allele-specific inactivation of HTT by targeting a protein coding sequence containing a common, heterozygous single nucleotide polymorphism (SNP). The outcome is a marked and allele-selective reduction of mutant HTT (mHTT) protein in a mouse model of HD. Expression of a single CRISPR-Cas9 nuclease in neurons generated a high frequency of mutations in the targeted HD allele that included both small insertion/deletion (InDel) mutations and viral vector insertions. Thus, allele-specific targeting of InDel and insertion mutations to heterozygous coding region SNPs provides a feasible approach to inactivate autosomal dominant mutations that cause genetic disease.

MAIN TEXT

INTRODUCTION

Huntington's disease (HD) is due to an autosomal dominant mutation in the huntingtin gene. In the mutant allele, a tandem CAG triplet repeat located in exon one is expanded to greater than 36 copies (Huntingtons Disease Collaborative, 1993). The resulting polyglutamine (polyQ) peptide in the mutant huntingtin protein (mHTT) is considered the initiating pathogenic molecule¹⁻³. A primary goal of therapy is to reduce mHTT mRNA and protein⁴. Various strategies have been described to reduce HTT protein, including blocking transcription of the mutant gene^{5,6}, and reducing mHTT mRNA using anti-sense oligonucleotides (ASOs), siRNAs, and virally-delivered miRNAs⁶⁻¹⁵. These approaches have potential caveats. Oligonucleotide therapies require multiple treatments and transcriptional inactivation requires persistent expression of an exogenous repressor. Another challenge is assessing the optimal degree of HTT reduction. Too little reduction of mHTT may be insufficient for clinical improvement while too great a reduction in normal HTT may have negative consequences. For example, in a clinical trial with HTT-lowering ASOs, the authors estimated that mHTT was reduced by 20-35% in striatum, but this intervention was insufficient to alter disease progression¹⁶.

CRISPR-Cas9 based gene editing^{17,18} provides an alternative approach to permanently prevent expression of the toxic mHTT protein. The nuclease complex is composed of a single guide RNA (sgRNA) that pairs with DNA and the Cas9 protein that binds a short DNA sequence and cleaves the target DNA site. Repair of the induced double strand DNA breaks can disrupt protein expression by generating small frameshift mutations at single target sites or large deletions between pairs of sites.

Gene editing may be useful for HD^{19,20}, but important limitations must be addressed. Given the permanent nature of DNA sequence changes and the essential role of HTT in the adult mouse brain²¹⁻²⁵, it is prudent to retain the normal HTT. Allele-specific targeting of HTT using CRISPR-Cas9 based nucleases can

distinguish between single nucleotide polymorphism (SNP) target sites^{19, 26, 27}.

Previous allele-specific editing used two target sites to make deletions that remove exon 1 or make large deletions elsewhere in the gene^{26, 27}. However, using two cut sites can limit the efficiency of mHTT disruption since InDel mutations or viral vector insertions at the individual target sites will compete with deletions between both sites²⁸⁻³⁰.

Here, we describe an alternative gene editing approach (**Figure 1**) with sgRNAs that target single SNP sites in the HTT protein coding regions¹⁰. We describe an sgRNA that efficiently edits the mutant allele, but cannot edit the normal allele due to a single mismatch to the sgRNA at the SNP. Unlike mutations in intronic, UTR regions or untranscribed regions, a single frameshift mutation or vector insertion in the coding region can disrupt gene expression by evoking cellular mRNA surveillance mechanisms that block or reduce expression of the encoded protein³¹. Using a mouse HD model with two human transgenes encoding mHTT and normal HTT, we demonstrate efficient, allele-specific reduction of mHTT protein in mouse striatum.

METHODS

Detailed experimental methods are provided in Supplemental File 6.

Guide RNA design

Target sites for the CRISPR-SpCas9 nuclease were designed using the opensource Bioconductor software package CRISPRseek³⁸. Htt-SNP targeting sgRNAs are listed in Supplemental Table 1.

In vitro validation of guide RNAs

HEK293T cells were co-transfected with a pM427 GFP reporter plasmid³² with the target site and a pX330 sgRNA plasmid³³ expressing sgRNA and Cas9. GFP expressing cells (were measured 48 hours post transfection by flow cytometry.

Lentivirus infections

sgRNAs were cloned into lentiCRISPRv2_CMVGFP plasmid (modified from Addgene, 82416)³⁴. High titer Lentivirus was produced as described previously³⁵. Human HD fibroblasts were infected at an MOI of 50 and analyzed after 7 days. Mouse primary neurons were infected five days after plating and harvested 7 days after infection. Editing efficiency, genotypes and sgRNAs were determined for each infection by PCR and Sanger sequencing.

Mice

The mouse model for allele-specific targeting of mHTT contains one transgene expressing mHTT (BAC97) and a second transgene expressing normal HTT (YAC18). The BAC97 transgenic mice (FVB/N-Tg(HTT*97Q)LXwy/Chdij) were obtained from William Yang at UCLA³⁶. BAC97 mice express a neuropathogenic, full-length human mutant Huntingtin gene modified to harbor a *loxP*-flanked human mutant *htt* exon 1 sequence containing 97 mixed CAA-CAG repeats. YAC18 transgenic mice (FVB/N-Tg(HTT*18Q)) were obtained from Michael Hayden at the University of British Columbia³⁷. YAC18 mice have a normal length human Huntingtin (18 polyglutamate repeats). Both the YAC18 and BAC97 mice were crossed to *Hdh*^{-/-} (Huntingtin null) mice³⁸ obtained from William Yang to produce YAC18 or BAC7, *Hdh*^{-/+} animals. A second cross produced YAC18 BAC97 mice with no endogenous mouse Huntingtin (YAC18 BAC97 *Hdh*^{-/-}). Repeat lengths were checked by PCR and sequencing to ensure that there was no genetic drift. Cas9 knock in mice³⁹ (Cas9: Gt(ROSA)26Sor/J) were obtained from Jackson labs and were crossed with BAC97 mice to produce BAC97 mice homozygous for Cas9. To generate YAC18 BAC97 mice with Cas9, BAC97 Cas9 homozygous mice were crossed with YAC18 mice (YAC18 BAC97 *Hdh*^{-/-} Cas9 het). All mice used in this study were housed in the University of Massachusetts vivarium on a 12/12 light cycle with free access to food and water. All animal protocols were approved in the University of Massachusetts Medical School's IACUC protocol # A978-18.

AAV injections of adult mouse brains

sgRNAs were cloned into the scAAV_CB6_TurboRFP_RBG vector. AAV Vectors were packaged into the AAV-AS serotype⁴⁰ by the UMASS Viral Vector Core. Virus was injected

in eight week old animals. The injection coordinates were measured from the bregma (1.0mm anterior, 2.0mm lateral and 3.0mm from the surface of the brain). Tissue was collected as a 2mm biopsy punch from striatal sections. Genotypes and virus were confirmed by PCR and Sanger sequencing. Editing efficiencies were surveyed by PCR and Sanger sequencing.

Illumina sequencing

Gene specific primers with TruSeq overhang sequences were used to amplify 150bp target sequences. Target regions were amplified using barcoded TruSeq primers. Paired-end sequences from pooled libraries were determined by the UMASS Medical School Deep Sequencing Core.

Sequence analysis

The CRISPResso software package⁴¹ quantified the frequency of each unmodified SNP allele and the frequency, size and position of induced InDel mutation. SNPclassifier, a custom python code, was used to assign InDel mutations to a parental SNP allele. Editing frequencies were also evaluated using Sanger sequences analyzed with the TIDE web tool (<https://tide.deskgen.com/>)⁴².

Protein analysis

Lysates were prepared from frozen tissue punches from one striatal hemisphere. HTT levels were characterized using a Simple Western assay (Wes, ProteinSimple). Western blots with these lysates were performed as previously described⁹.

Conventional and Droplet Digital PCR to detect viral insertions

The primers and probes used for conventional and droplet digital PCR to detect viral insertions are listed in the Key Resources Table. For conventional PCR approximately 100ng of template genomic DNA was amplified with Phusion High Fidelity polymerase. Droplet digital PCR reactions were performed using Droplet Digital PCR Supermix and droplets were generated and analyzed with the QX200 Droplet Digital PCR System (BioRad).

Immunohistochemistry for DARPP32 and IBA1

40 micrometers sections were prepared from treated and control animals. Every fifth section was used for immunohistochemistry staining. Sections were stained with anti-DARPP rabbit monoclonal antibody or anti-IBA1 antibody. Numbers of positively stained cells were determined for each animal using 50 images from 5 sections.

Quantification and Statistical Analysis

Linear regression was used to quantify and test the statistical significance between treatment conditions within genotype or treatment duration and between genotype or treatment duration within treatment groups. Analyses were conducted using STATA (v16) software's regression command to fit models for each dependent variable then using post-estimation contrasts to test each hypothesis. We considered p-values less than 0.05 to be statistically significant.

RESULTS

Allele-specific nucleases can target common HTT SNP heterozygosities

We previously developed a computational tool⁴³ to identify candidate allele-specific gRNAs. An example is diagrammed with an sgRNA that targets the "T" allele of a SNP heterozygosity in exon 50 (**Figure 1**). The non-targeted "C" allele has a mismatch to the hybridizing sgRNA. We used a GFP reporter assay³² to identify gRNAs with high activity for the targeted SNP allele and low activity for the other allele (**Supplemental Table 1, Supplemental Figure 1**), including allele-specific gRNAs targeting SNPs in exons 48, 50 and 57.

Allele-specific gene editing reduces mutant HTT in mouse primary neurons

We tested gene editing at protein coding region SNPs for allele-specific reduction of mHTT protein in neurons. We focused on the Ex50T-g1 gRNA targeting the T allele of SNP RS362331 in exon 50. RS362331 is the most frequently heterozygous protein coding region SNP in HD patients¹⁰ and the T allele is more frequently associated with the mutant HTT haplotype⁴⁴.

Primary cortical neurons were derived from a mouse model with two human HTT transgenes (**Figure 2**). The BAC97 transgene³⁶ encodes a mHTT protein with 97 glutamine codons and has the “T” allele at the exon 50 SNP. The YAC18 transgene³⁷ expresses normal HTT and has the “C” allele. The mice were also homozygous for a null mutation of the endogenous mouse HTT gene³⁸ and expressed transgenic Cas9³⁹. An sgRNA targeting the T allele at exon 50 (Ex50T) was delivered to primary neurons by lentiviral transduction 5 days after isolation and cells were harvested one week later (**Figure 2A**). An sgRNA targeting the mouse Rosa26 locus was used as a control.

Edited genomic DNA sequences from the exon 50 SNP region were determined by Illumina sequencing of PCR amplicons. In control samples, the “T” allele present in the BAC97 transgene was present in 81% of sequences and the C allele from the YAC18 transgene was present in 19%, reflecting a higher copy number for the BAC97 transgene (**Figure 2B**). In Ex50Tg1 treated neurons, sequences with the unaltered “T” allele were reduced from 81% to 29%, while sequences harboring induced InDel mutations rose to 40%, suggesting that the InDel mutations result from inaccurate repair of DNA breaks at the targeted “T” allele. Greater than 90% of the observed InDel mutations are frameshift mutations with the most frequent allele being the addition of a single C nucleotide (**Figure 2C, Supplemental Figure 2**).

For many InDel mutations, the polymorphic base from SNP RS362331 is still present, allowing the InDel to be attributed to one of the two parental alleles. For example, the single C insertion is associated with the T allele of the SNP (**Supplemental Figure 2, Ex50Tg1 treated, third line**). In contrast, the provenance of some alleles cannot be determined due to deletion of the diagnostic SNP (**Supplemental Figure 2, Ex50Tg1 treated, seventh line**). A custom software tool (SNPclassifier, **Supplemental File 2**) was created that assigned all alleles either to the parental T allele, or the parental C allele, or to an undetermined category. The nearly all InDel mutations in primary neurons treated with the Ex50T gRNA were

either associated with the parental T allele or could not be assigned (**Supplemental Table 2**).

Our gene editing approach reduced full length mHTT protein (from BAC97) with no detectable change in the non-targeted normal HTT protein (from YAC18) (**Figure 3A, B**). Although the frameshift mutations are induced in exon 50, smaller HTT protein fragments were not detected by Western blot analysis (**Figure 3C**). Thus, allele-specific targeting of a HTT coding region SNP reduced mutant, but not normal HTT protein in primary neurons.

Gene editing at SNP heterozygosities selectively lowers mHTT in mouse striatum

We tested *in vivo* gene editing of mHTT in the striatum of adult BAC97/YAC18/Cas9 mice (**Figure 4**). The Ex50Tg1 sgRNA was delivered using an AAV vector⁴⁰ that expresses the sgRNA (**Figure 4A**). AAV expressing an sgRNA targeting the Rosa26 locus was used as control. Vector was introduced by injection into the adult mouse striatum. Twenty-nine, thirty-seven and thirty-three percent InDels were observed at 2, 4 and 6 weeks following injection. Ninety-three percent of the InDels were frameshift mutations. The increase in InDels was accompanied by a reduction in the targeted BAC97 (**Figure 4B**). To determine if InDels could be induced in the non-targeted YAC18 transgene in the absence of BAC97, animals transgenic for only the YAC18 and Cas9 transgenes were injected AAV expressing either Ex50Tg1 or Rosa26 control sgRNAs. Four weeks following injection, InDel mutation rates were determined by TIDE analysis of Sanger sequencing chromatograms⁴²; the signal in Ex50Tg1 treated tissue (2.1 percent, S.E.M = 1.0 percent) was no higher than the background signal in Rosa26 treated controls (3.5 percent, S.E.M. = 2.3 percent). Thus, brief expression of CRISPR-Cas9 gene editing complexes in cultured neurons or extended expression in adult brain tissue induced frameshift mutations in the targeted mutant allele without altering the non-targeted allele.

Frameshift mutations in protein coding sequences can evoke RNA surveillance mechanisms that prevent translation of mRNAs with premature termination codons^{31, 45}. We examined whether there was an allele-specific reduction in mHTT

RNAs 4 weeks after editing. RT-PCR followed by Illumina sequencing was used to determine the relative frequencies of each HTT exon 50 SNP allele and of induced InDels from AAV-treated striatum. Twenty-five percent of sequences in treated samples were InDel mutations (**Supplemental Figure 5, exon 50**). The targeted BAC97 mHTT allele decreased from 68 percent in controls to 18 percent with Ex50T gRNA. Together, the frequency of all exon 50 cDNA sequences from mHTT (BAC97 sequences plus InDels) was reduced from 68% to 43%, consistent with degradation of mHTT mRNA. The relative amounts of mHTT versus wild type HTT RNA were also assayed by sequencing heterozygous SNPs at exons 48 and 57. In cDNA sequences, the frequency of BAC97 alleles was reduced at both flanking exons (**Supplemental Figure 5, exons 48 and 57**), indicating that mHTT RNA was reduced.

We examined allele-specific reduction of mHTT protein at 4 and 6 weeks following sgRNA delivery to the striatum. The targeted mHTT protein (from BAC97) decreased approximately 4-fold, while wild type HTT (from YAC18) was not reduced (**Figure 5, Supplemental Figure 3**). Truncated HTT protein products were not detected (**Supplemental Figure 4**).

To test if either AAV delivery or CRISPR-Cas9 editing at mHTT was toxic, we examined levels of DARPP32, which is highly enriched in striatal neurons, and GFAP, which is a glial marker that increases during stress. There were no changes in either after mHTT lowering (**Supplemental Figure 7**). Immunohistochemical analysis of Iba1, a marker of microglia, only revealed increased staining directly adjacent to the needle injection site (**Supplemental Figure 6C, n = 3**). The total number of immunoreactive Iba1-positive microglia and DARPP32-positive neurons and were not different between treatment groups (**Supplemental Figure 6D, E**).

AAV and lentiviral mediated gene editing generates non-amplifiable alleles and viral vector insertions

Amplicon sequencing of treated primary neurons showed an increase in the percent of YAC18 alleles (**Figure 2**). This increase could occur if some editing-induced mutations in the BAC97 allele prevent PCR amplification (**Figure 6A**). We

quantified the fraction of HTT exon 50 sequences that could no longer be amplified using droplet digital PCR^{46, 47}. Paired samples were obtained by treating primary neurons derived from individual animals with either control or Ex50T gRNAs. The human HTT exon 50 copy number was decreased by an average of 44% in Ex50T-treated versus control cells (**Figure 6D**).

The estimated fraction of non-amplifiable alleles was added to the sequenced alleles from Figure 2B to infer the actual fraction of each allele class (**Figure 6E**). After including 44% non-amplified alleles in treated samples, the inferred frequency of unaltered BAC97 alleles was 16% in Ex50T treated samples. The inferred frequency of induced InDel mutations was 22%. Together, the frequency of non-amplified alleles plus InDel mutations represented 66% of alleles in the treated sample. In this analysis, the non-targeted YAC18 alleles were unchanged by editing, remaining at 18%. Editing in the striatum generated a similar result (**Figure 6F, G**). Thus, in both primary neurons and striatum, AAV delivery of sgRNAs induced a combination of InDel mutations, which were included in our sequenced alleles, and an additional class of mutations that were not represented in the sequenced amplicons. The relative frequency of each of these classes can be inferred by ddPCR quantification of the missing alleles.

To determine if very large deletions were removing the BAC97 allele at exon 50, we examined the frequency of SNP heterozygosities at flanking exons 48 and 57. There was no significant change in the BAC97 or YAC18 allele at either flanking SNP site (**Figure 4C**), indicating that the mutations that prevent amplification were not large deletions.

Previous studies reported that AAV-mediated delivery of CRISPR-Cas9 generate a high rate of AAV insertions, including in normal mouse brain^{28, 29}. PCR analysis revealed lentiviral and AAV insertions at the human HTT exon 50 locus or the control Rosa26 locus following gRNA delivery (**Supplemental Figure 8**). Insertions were only detected at the site targeted by the corresponding gRNA, demonstrating that delivery of gene editing components by lentivirus or AAV induces viral insertion mutations at the target site.

Allele-specific editing of coding SNPs in HD patient-derived fibroblasts.

To confirm allele-specific targeting in human cells, we used HD patient derived fibroblasts heterozygous for the common HTT coding region SNPs. Unlike post-mitotic neurons, fibroblasts can use the non-targeted allele to repair induced DNA breaks; this homology-dependent repair would increase the frequency of the non-targeted allele. Untreated fibroblasts had an equal frequency of each allele. Treated fibroblasts exhibited induced InDels (19%), decrease of the targeted allele (50% to 7%), and an increase in the non-targeted allele (50 to 74%). Sequencing of the individual alleles revealed that most or all InDels were derived from the targeted allele (**Supplemental Figure 9**). These results confirm allele-specificity in HD patient derived cells.

Analysis of Off-target sites

We characterized potential off-target sites for the Ex50Tg1 gRNA in the human genome. Loci with up to three mismatches to the target sequence were sequenced from HEK293T cells treated with ribonucleoprotein (RNP) complexes programmed with either Ex50Tg1 or a control gRNA. Eighty-seven percent of HTT sequences contained InDels at the targeted sequence (Supplemental File 7). Among the predicted off-target sites, a single site had InDels above the detection limit of 0.15% in two replicates. This site, in an intronic sequence, exhibited a 0.9% and 1.5% editing rate in this experiment.

DISCUSSION

A critical challenge for developing therapeutics for autosomal dominant disorders such as HD is to reduce the activity of the mutant protein while preserving normal protein function. We demonstrate the usefulness of CRISPR-Cas gene editing at a protein coding region SNP with high heterozygosity in the HD population.

Compared with previous editing studies using mouse models of HD, our approach has some possible problems and potential advantages. Elimination of the expanded CAG repeat region is the most straightforward way to prevent mHTT toxicity and previous studies have demonstrated that one or two gRNAs targeting the coding

region of exon 1 of a mHTT transgene can rescue organismal phenotypes^{19, 48}. However, neither of these studies uses an allele-specific approach. In another study²⁶, allele-specific gRNAs targeted regions flanking exon 1, but only an estimated 20% of HD patients are estimated to be heterozygous at both sites. In addition, these sgRNAs also reduced expression of the endogenous mouse htt gene²⁶, so whether they would be allele-specific in a model such as the BAC97/YAC18 used in our study is unclear. Our study is the first demonstration of allele-specific knockdown of mHTT in a mouse model with two human transgenes expressing both mHTT and normal HTT. Furthermore, a significant percentage of HD patients are candidates for this approach. SNP RS362331 is heterozygous in 40 to 46% of HD patients^{10, 49}. Targeting three coding region SNPs using our strategy should enable treatments for 70 to 80% of patients^{10, 43}.

A second advantage of allele-specific targeting of HTT at single coding region sites is that both InDels and vector insertions can disrupt gene function. A possible limitation of creating deletions between two target sites is that the frequent induction of viral insertions or InDel mutations at one or both sites will prevent the formation of deletions between the two sites²⁸. The *in vivo* frequencies of these different outcomes can be challenging to measure and were not tested in the previous mouse study of allele-specific editing²⁶. In contrast, when targeting single SNP heterozygosities that occur within the protein coding region, either individual InDel mutations or other mutations such as large insertions or deletions are sufficient to reduce protein levels. Our results targeting a single coding region SNP heterozygosity demonstrates a high efficiency of allele-specific reduction of the targeted gene. The 40-50% reduction of mHTT protein we observed when targeting a SNP in exon 50 is similar to that described using one or two sgRNAs to target the non-polymorphic regions of exon 1^{19, 48}.

An unexpected outcome of our analysis was the increase in the percentage of sequence reads with the non-targeted allele in treated neurons (the YAC18 allele in Figures 2B and 4B). In dividing cells, this increase could reflect homology-dependent repair of the targeted allele using the non-targeted allele as a donor.

However, homology-dependent repair is low or absent in most post-mitotic cells such as neurons. We found that most induced mutations were excluded from our sequence analysis (Figure 6). If these “unamplified” alleles were added to the sequenced alleles, the non-targeted alleles were unchanged after gene editing (Figures 6E and G). Recent studies suggest that a combination of AAV vector insertions, large deletions or other rearrangements can comprise a major fraction of edited alleles when AAV is used to deliver gene editing components²⁸⁻³⁰. In our experiments, most mutations induced by AAV or by lentivirus delivery of sgRNAs were not amplified using primers that flank the targeted site. With both AAV and lentivirus, the viral vector sequences were found at the CRISPR-Cas9 targeted site. These results suggest that many gene editing experiments using either lentivirus or AAV have the potential for frequent viral insertions at the targeted site. While AAV and integrase-defective lentivirus were known to insert at sites of induced DNA breaks, this is, to the best of our knowledge, the first demonstration that integration-competent lentivirus, which typically integrates at random genomic sites, was directed to integrate at DNA breaks induced by CRISPR-Cas9 gene editing. Depending on the types of sequences carried by the viral vector, such insertions might result in a different cellular outcome than would be expected with a simple InDel or deletion allele.

The terminal regions of both viral vectors used in this study have stop codons in all three reading frames; when these sequences insert at the exon 50 editing site, they are predicted to result in a truncated mHTT protein coding region. For the HTT locus, we demonstrated that while there are both the expected InDel mutations and unanticipated viral insertions, the outcome of editing at the exon 50 SNP is a significant reduction in full length HTT protein and no detectable truncated products. These results suggest that either InDel or insertion mutations result in altered RNA and/or protein products with reduced expression.

For clinical applications of the approach described here, improvements in specificity and delivery are needed. We detected low rates of editing at one potential off-target site; one possible way to reduce off-target editing is use of

higher fidelity editing enzymes⁵⁰. In addition, alternative methods for gRNA and Cas9 delivery are required. For *in vivo* expression of Cas9 in mice, we have taken advantage of a Cas9 transgene; however, previous HTT studies have confirmed that it is possible to deliver both sgRNAs and SpCas9 using two AAV viruses or sgRNAs with SaCas9 using a single AAV virus^{19, 48}. In addition to viral delivery, future therapeutic implementation of allele-specific editing may deliver transient editing complexes containing gRNAs with Cas9 mRNA or gRNAs with Cas9 protein, which could lower off-target activity and improve *in vivo* safety⁵¹.

CONCLUSION

We conclude that using viral delivery to target coding region SNPs for gene editing is a viable approach to selectively reduce mutant HTT protein expression.

ACKNOWLEDGEMENTS

The authors would like to thank David Howland and Richard Chen of the CHDI Foundation for their support and scientific insights. The authors also thank Wendy Cullinane and Rina Paladino for administrative support. Illumina sequencing was performed at the University of Massachusetts Medical School Deep Sequencing Core.

AUTHOR CONTRIBUTIONS

SRO, ELP, MSE, SAW, MD, NA, MHB conceived and planned experiments. SRO, ELP, ES, KOC, LAK, EH, RM, and AC carried out the experiments. SRO, LJZ, EOM, MD and MHB analyzed the data. SRO, NA, and MHB wrote the manuscript, with feedback from all authors.

AUTHOR DISCLOSURE STATEMENT

The authors declare no competing interests.

FUNDING STATEMENT

This work was supported by NIH R01 NS106245 to MHB and NA, CHDI Foundation Research Agreement A-10199 to MHB, CHDI Foundation Research Agreement A-5038 to NA, CHDI Research Agreement A-6367 to MD, the Dake Family Fund to MD

and NIH UL1 TR000161-05 to the University of Massachusetts Center for Clinical and Translation Science.

REFERENCES

1. HuntingtonsDiseaseCollaborative. A novel gene containing a trinucleotide repeat that is expanded and unstable on Huntington's disease chromosomes. *Cell* 1993;72:971-983.
2. Aronin N, Chase K, Young C et al. CAG expansion affects the expression of mutant Huntingtin in the Huntington's disease brain. *Neuron* 1995;15:1193-1201.
3. DiFiglia M, Sapp E, Chase K et al. Huntingtin is a cytoplasmic protein associated with vesicles in human and rat brain neurons. *Neuron* 1995;14:1075-1081.
4. Sah DW, Aronin N. Oligonucleotide therapeutic approaches for Huntington disease. *The Journal of clinical investigation* 2011;121:500-507.
5. Garriga-Canut M, Agustin-Pavon C, Herrmann F et al. Synthetic zinc finger repressors reduce mutant huntingtin expression in the brain of R6/2 mice. *Proc Natl Acad Sci U S A* 2012;109:E3136-3145.
6. Zeitler B, Froelich S, Marlen K et al. Allele-selective transcriptional repression of mutant HTT for the treatment of Huntington's disease. *Nat Med* 2019;25:1131-1142.
7. Kordasiewicz HB, Stanek LM, Wancewicz EV et al. Sustained therapeutic reversal of Huntington's disease by transient repression of huntingtin synthesis. *Neuron* 2012;74:1031-1044.
8. Pfister EL, DiNardo N, Mondo E et al. Artificial miRNAs Reduce Human Mutant Huntingtin Throughout the Striatum in a Transgenic Sheep Model of Huntington's Disease. *Hum Gene Ther* 2018;29:663-673.
9. Keeler AM, Sapp E, Chase K et al. Cellular Analysis of Silencing the Huntington's Disease Gene Using AAV9 Mediated Delivery of Artificial Micro RNA into the Striatum of Q140/Q140 Mice. *J Huntingtons Dis* 2016;5:239-248.
10. Pfister EL, Kennington L, Straubhaar J et al. Five siRNAs targeting three SNPs may provide therapy for three-quarters of Huntington's disease patients. *Current biology : CB* 2009;19:774-778.

11. Harper SQ, Staber PD, He X et al. RNA interference improves motor and neuropathological abnormalities in a Huntington's disease mouse model. *Proc Natl Acad Sci U S A* 2005;102:5820-5825.
12. Alterman JF, Godinho B, Hassler MR et al. A divalent siRNA chemical scaffold for potent and sustained modulation of gene expression throughout the central nervous system. *Nat Biotechnol* 2019;37:884-894.
13. Evers MM, Miniarikova J, Juhas S et al. AAV5-miHTT Gene Therapy Demonstrates Broad Distribution and Strong Human Mutant Huntingtin Lowering in a Huntington's Disease Minipig Model. *Mol Ther* 2018;26:2163-2177.
14. Miniarikova J, Zimmer V, Martier R et al. AAV5-miHTT gene therapy demonstrates suppression of mutant huntingtin aggregation and neuronal dysfunction in a rat model of Huntington's disease. *Gene Ther* 2017;24:630-639.
15. Stanek LM, Sardi SP, Mastis B et al. Silencing mutant huntingtin by adeno-associated virus-mediated RNA interference ameliorates disease manifestations in the YAC128 mouse model of Huntington's disease. *Hum Gene Ther* 2014;25:461-474.
16. Smith AV, Tabrizi SJ. Therapeutic Antisense Targeting of Huntingtin. *DNA Cell Biol* 2020;39:154-158.
17. Heidenreich M, Zhang F. Applications of CRISPR-Cas systems in neuroscience. *Nat Rev Neurosci* 2016;17:36-44.
18. Hsu PD, Lander ES, Zhang F. Development and applications of CRISPR-Cas9 for genome engineering. *Cell* 2014;157:1262-1278.
19. Yang S, Chang R, Yang H et al. CRISPR/Cas9-mediated gene editing ameliorates neurotoxicity in mouse model of Huntington's disease. *The Journal of clinical investigation* 2017;127:2719-2724.
20. Merienne N, Vachey G, de Longprez L et al. The Self-Inactivating KamiCas9 System for the Editing of CNS Disease Genes. *Cell Rep* 2017;20:2980-2991.

21. Liu JP, Zeitlin SO. Is Huntingtin Dispensable in the Adult Brain? *J Huntingtons Dis* 2017;6:1-17.
22. Burrus CJ, McKinstry SU, Kim N et al. Striatal Projection Neurons Require Huntingtin for Synaptic Connectivity and Survival. *Cell Rep* 2020;30:642-657 e646.
23. Dragatsis I, Levine MS, Zeitlin S. Inactivation of Hdh in the brain and testis results in progressive neurodegeneration and sterility in mice. *Nat Genet* 2000;26:300-306.
24. Mehler MF, Petronglo JR, Arteaga-Bracho EE et al. Loss-of-Huntingtin in Medial and Lateral Ganglionic Lineages Differentially Disrupts Regional Interneuron and Projection Neuron Subtypes and Promotes Huntington's Disease-Associated Behavioral, Cellular, and Pathological Hallmarks. *J Neurosci* 2019;39:1892-1909.
25. McKinstry SU, Karadeniz YB, Worthington AK et al. Huntingtin is required for normal excitatory synapse development in cortical and striatal circuits. *J Neurosci* 2014;34:9455-9472.
26. Monteys AM, Ebanks SA, Keiser MS et al. CRISPR/Cas9 Editing of the Mutant Huntingtin Allele In Vitro and In Vivo. *Mol Ther* 2017;25:12-23.
27. Shin JW, Kim KH, Chao MJ et al. Permanent inactivation of Huntington's disease mutation by personalized allele-specific CRISPR/Cas9. *Hum Mol Genet* 2016.
28. Nelson CE, Wu Y, Gemberling MP et al. Long-term evaluation of AAV-CRISPR genome editing for Duchenne muscular dystrophy. *Nat Med* 2019;25:427-432.
29. Hanlon KS, Kleinstiver BP, Garcia SP et al. High levels of AAV vector integration into CRISPR-induced DNA breaks. *Nat Commun* 2019;10:4439.
30. McCullough KT, Boye SL, Fajardo D et al. Somatic Gene Editing of GUCY2D by AAV-CRISPR/Cas9 Alters Retinal Structure and Function in Mouse and Macaque. *Hum Gene Ther* 2019;30:571-589.
31. Popp MW, Maquat LE. Organizing principles of mammalian nonsense-mediated mRNA decay. *Annual review of genetics* 2013;47:139-165.

32. Wilson KA, Chateau ML, Porteus MH. Design and Development of Artificial Zinc Finger Transcription Factors and Zinc Finger Nucleases to the hTERT Locus. *Mol Ther Nucleic Acids* 2013;2:e87.
33. Cong L, Ran FA, Cox D et al. Multiplex genome engineering using CRISPR/Cas systems. *Science* 2013;339:819-823.
34. Walter DM, Venancio OS, Buza EL et al. Systematic In Vivo Inactivation of Chromatin-Regulating Enzymes Identifies Setd2 as a Potent Tumor Suppressor in Lung Adenocarcinoma. *Cancer Res* 2017;77:1719-1729.
35. Sena-Esteves M, Tebbets JC, Steffens S et al. Optimized large-scale production of high titer lentivirus vector pseudotypes. *J Virol Methods* 2004;122:131-139.
36. Gray M, Shirasaki DI, Cepeda C et al. Full-length human mutant huntingtin with a stable polyglutamine repeat can elicit progressive and selective neuropathogenesis in BACHD mice. *J Neurosci* 2008;28:6182-6195.
37. Hodgson JG, Agopyan N, Gutekunst CA et al. A YAC mouse model for Huntington's disease with full-length mutant huntingtin, cytoplasmic toxicity, and selective striatal neurodegeneration. *Neuron* 1999;23:181-192.
38. Zeitlin S, Liu JP, Chapman DL et al. Increased apoptosis and early embryonic lethality in mice nullizygous for the Huntington's disease gene homologue. *Nat Genet* 1995;11:155-163.
39. Platt RJ, Chen S, Zhou Y et al. CRISPR-Cas9 knockin mice for genome editing and cancer modeling. *Cell* 2014;159:440-455.
40. Choudhury SR, Harris AF, Cabral DJ et al. Widespread Central Nervous System Gene Transfer and Silencing After Systemic Delivery of Novel AAV-AS Vector. *Mol Ther* 2016;24:726-735.
41. Pinello L, Canver MC, Hoban MD et al. Analyzing CRISPR genome-editing experiments with CRISPResso. *Nat Biotechnol* 2016;34:695-697.

42. Brinkman EK, van Steensel B. Rapid Quantitative Evaluation of CRISPR Genome Editing by TIDE and TIDER. *Methods Mol Biol* 2019;1961:29-44.
43. Zhu LJ, Holmes BR, Aronin N et al. CRISPRseek: a bioconductor package to identify target-specific guide RNAs for CRISPR-Cas9 genome-editing systems. *PloS one* 2014;9:e108424.
44. Chao MJ, Gillis T, Atwal RS et al. Haplotype-based stratification of Huntington's disease. *Eur J Hum Genet* 2017;25:1202-1209.
45. Palacios IM. Nonsense-mediated mRNA decay: from mechanistic insights to impacts on human health. *Briefings in functional genomics* 2013;12:25-36.
46. Hatch AC, Fisher JS, Tovar AR et al. 1-Million droplet array with wide-field fluorescence imaging for digital PCR. *Lab Chip* 2011;11:3838-3845.
47. Hindson BJ, Ness KD, Masquelier DA et al. High-throughput droplet digital PCR system for absolute quantitation of DNA copy number. *Anal Chem* 2011;83:8604-8610.
48. Ekman FK, Ojala DS, Adil MM et al. CRISPR-Cas9-Mediated Genome Editing Increases Lifespan and Improves Motor Deficits in a Huntington's Disease Mouse Model. *Mol Ther Nucleic Acids* 2019;17:829-839.
49. Lombardi MS, Jaspers L, Spronkmans C et al. A majority of Huntington's disease patients may be treatable by individualized allele-specific RNA interference. *Exp Neurol* 2009;217:312-319.
50. Vakulskas CA, Dever DP, Rettig GR et al. A high-fidelity Cas9 mutant delivered as a ribonucleoprotein complex enables efficient gene editing in human hematopoietic stem and progenitor cells. *Nat Med* 2018;24:1216-1224.
51. van Haasteren J, Li J, Scheideler OJ et al. The delivery challenge: fulfilling the promise of therapeutic genome editing. *Nat Biotechnol* 2020;38:845-855.

CORRESPONDENCE ADDRESS

Michael H. Brodsky

Department of Molecular Cell and Cancer Biology

University of Massachusetts Medical School, Worcester, MA 01605

michael.brodsky@umassmed.edu

Neil Aronin

Department of Medicine, RNA Therapeutics Institute

University of Massachusetts Medical School, Worcester, MA 01605

neil.aronin@umassmed.edu

FIGURE LEGENDS

Figure 1.

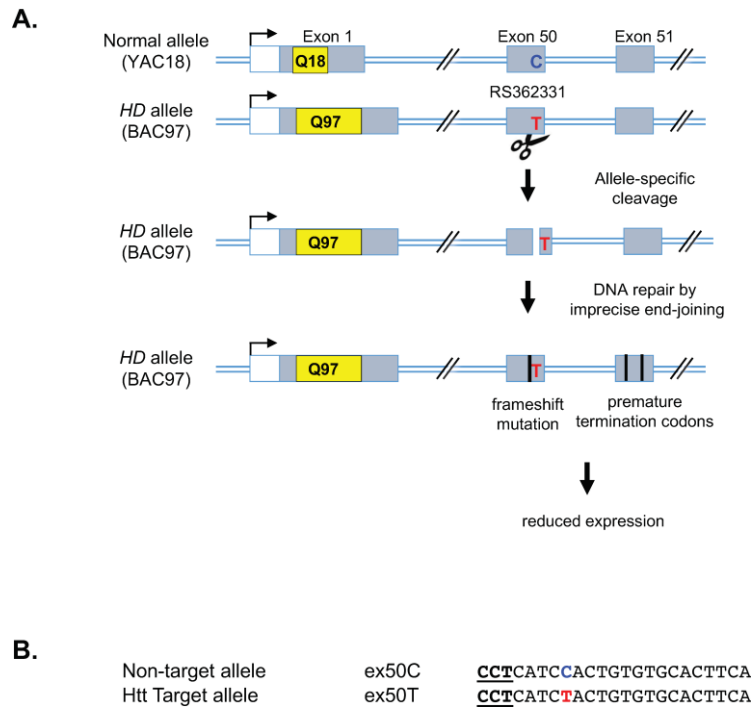
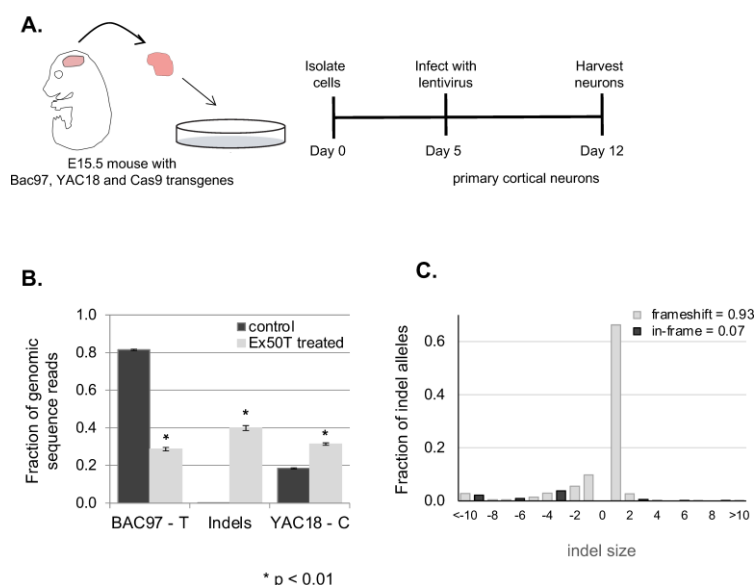


Figure 1. Strategy for allele-specific targeting of mutant HTT protein by gene editing. **A.** A strategy for allele-specific degradation of mutant Htt with SNP-specific nucleases. A schematic of the Htt gene depicts 3 of the 67 exons (not drawn to scale). Exon 1 can have a variable number of CAG repeats (indicated in yellow). HD results when a single copy of the gene has a repeat number greater than 36. To specifically alter the disease allele, an allele-specific gRNA-Cas9 nuclease targets a SNP that is heterozygous in an HD individual. In a mouse model of HD, the YAC18 transgene carries a normal version of the human HTT locus with the C allele of SNP RS362331 and the BAC97 transgene carries a mutant human HTT locus and the T allele of SNP RS362331. DNA cleavage and imprecise repair at the mutant HTT gene results in frameshift mutations that disrupt the coding region of the HD allele. Premature stop codons can reduce expression of the entire HTT protein, possibly through nonsense-mediated decay of the mature mRNA. **B.** CRISPR-Cas9 target sequences specific for two alleles of exon 50 are shown. The heterozygous SNP is shown in blue or red. The PAM sequence is in bold.

Figure 2.

**Figure 2. Allele-specific targeting of mHTT in BAC97/YAC18 primary neurons. A.**

Cartoon depicting the generation and infection of primary cortical neurons from mice heterozygous for Yac18 (wt) and Bac97 (mutant) human transgenes as well as a Cas9 transgene. **B.** An allele-specific sgRNA targeting the T allele of Htt Exon 50 (Ex50T) was introduced into BAC97/YAC18/Cas9 mouse primary neurons by lentiviral transduction using the LentiCRISPRcmvGFP vector. An sgRNA targeting the Rosa26 locus was used as a control. Genomic DNA was prepared 7 days following infection. PCR amplicons containing the targeted SNPs were barcoded and analyzed by Illumina sequencing. Insertion and deletion (InDel) allele frequencies were determined using the CRISPResso software package. The control sample has a higher frequency of the BAC97 allele than YAC18 due to a higher copy number of the BAC97 transgene. In the treated sample, 40% of reads are induced InDel mutations. N=3 mice and error bars represent the S.E.M. p-values less than 0.05 were considered significant. Exact p-values are reported in Supplemental File 3. **C.** The distribution of InDel sizes shows a strong bias towards frameshift mutations (filled bars) rather than in frame mutations (open bars). The insertion of a single base is the dominant allele type.

Figure 3.

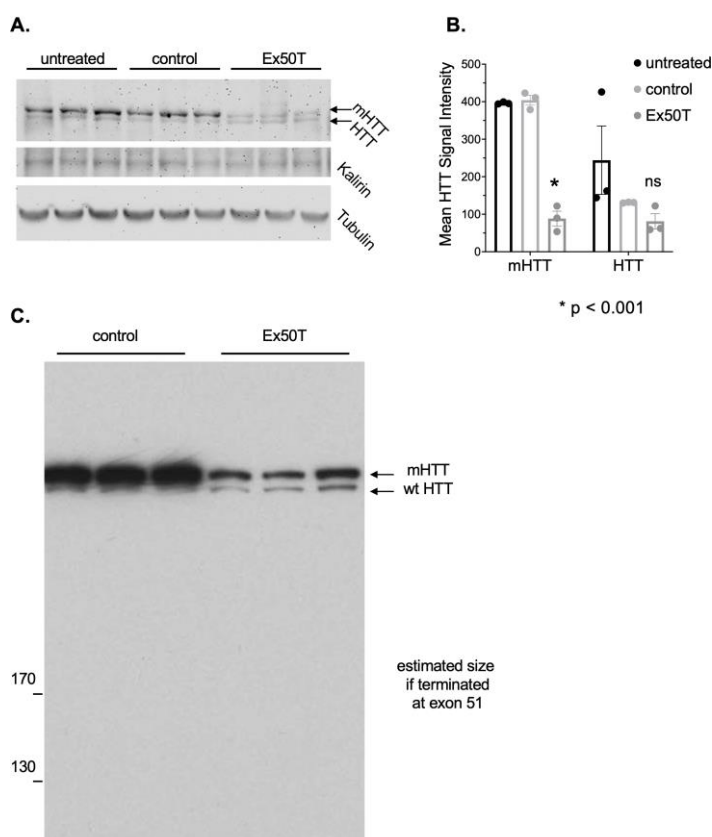


Figure 3. Allele-specific reduction of mutant HTT protein in primary neurons from a HD mouse. **A.** Mutant HTT (mHTT) and normal HTT protein were assayed following treatment with sgRNAs targeting Exon 50 (Ex50Tg1) or a Rosa26 (control). mHTT is expressed from the BAC97 transgene and normal HTT protein is expressed from the YAC18 transgene. mHTT runs at a higher molecular weight due to the increased size of the poly Q repeat sequence (upper blot). Higher mHTT protein expression is observed because of the higher transgene copy number. Kalirin and beta-tubulin provide total protein concentration controls. The targeted mHTT protein, but not normal HTT protein, is reduced when targeted with sgRNA Ex50Tg1. **B.** Quantification of HTT protein levels from digital images of the blot in A. mHTT and HTT signals are normalized to Kalirin levels. $n = 3$. Error bars indicate the S.E.M. Exact p-values are reported in Supplemental File 3. **C.** An additional protein gel was overexposed to detect accumulation of truncated protein products corresponding to translational termination following frameshift mutations in exon 50.

Figure 4.

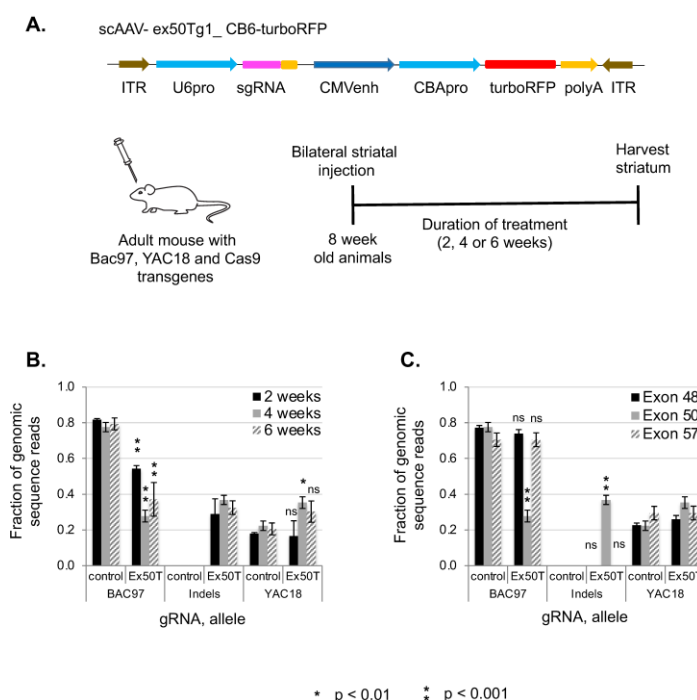


Figure 4. Allele-specific CRISPR-Cas9 targeting of HTT SNPs in the adult striatum of a mouse model of HD. **A.** Cartoon depicting the AAV vector used to deliver the Exon50Tg1 and control sgRNAs and the delivery of AAV to mouse brains. The HD model mice have two alleles at the exon50 SNP - the BAC97 transgene with the T allele and the YAC18 transgene with the C allele. The Ex50Tg1 sgRNA targets the T allele of the SNP heterozygosity. The gRNA and a turboRFP reporter gene are delivered by AAV injection into the adult striatum of 8-week-old mice. Cas9 activity is provided as a mouse transgene. **B.** Analysis at multiple time points. At two, four and six weeks following AAV treatment, the frequency of the BAC97 allele is reduced and InDel mutations are induced by the Ex50T programmed nuclease. **C.** Analysis of flanking exons. Heterozygous SNPs were examined by Illumina sequencing at two flanking exons in the 4 weeks samples. There is no significant change in the ratio of BAC97 to YAC18 alleles in exons 48 or 57, indicating that cleavage and repair at exon 50 does not induce a high frequency of deletions large enough to remove these SNPs. N=3 mice and error bars represent the S.E.M. p-values less than 0.05 were considered significant. Exact p-values are reported in Supplemental File 3.

Figure 5.

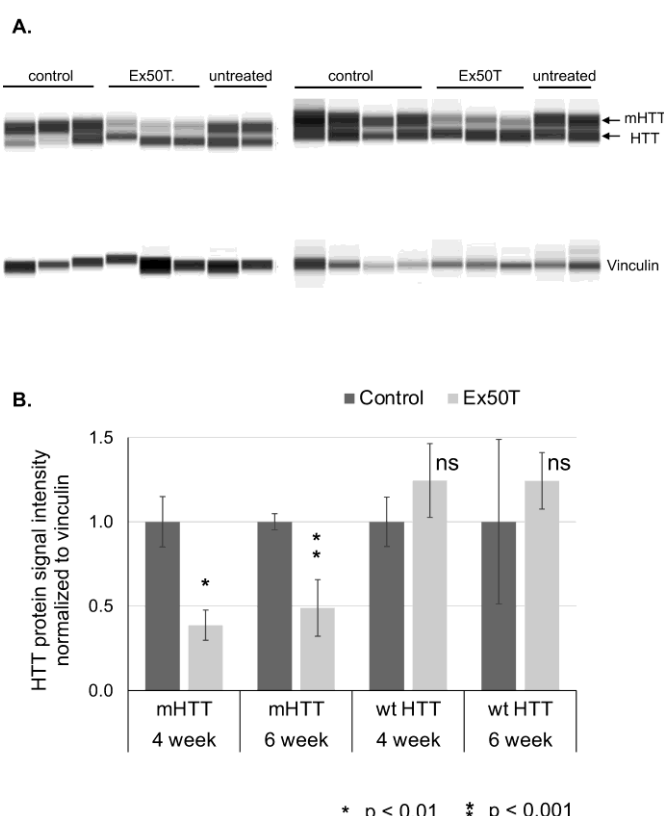


Figure 5. Allele-specific reduction of mHTT protein in the mouse adult striatum. A.

Protein sample analysis of HTT and mHTT protein from the striatum of HD model mice with the Cas9, BAC97 and YAC18 transgenes. Each animal was bilaterally injected with AAV expressing the control (Rosa26) or Ex50Tg1 sgRNAs. Protein was isolated from striatal tissue. Vinculin serves as a total protein control. Signal is visualized as a virtual blot format. **B.** Quantitative WES signals for mHTT and wild type HTT were normalized to vinculin. Each pair of control and Ex50T treated samples were further adjusted such that the control has a value of one. At both 4- and 6-weeks following injection with AAV expressing sgRNA Ex50T, mHTT was reduced by over 50% while wild type HTT was not significantly changed. N=3 mice and error bars represent the S.E.M. p-values less than 0.05 were considered significant. Exact p-values are reported in Supplemental File 3.

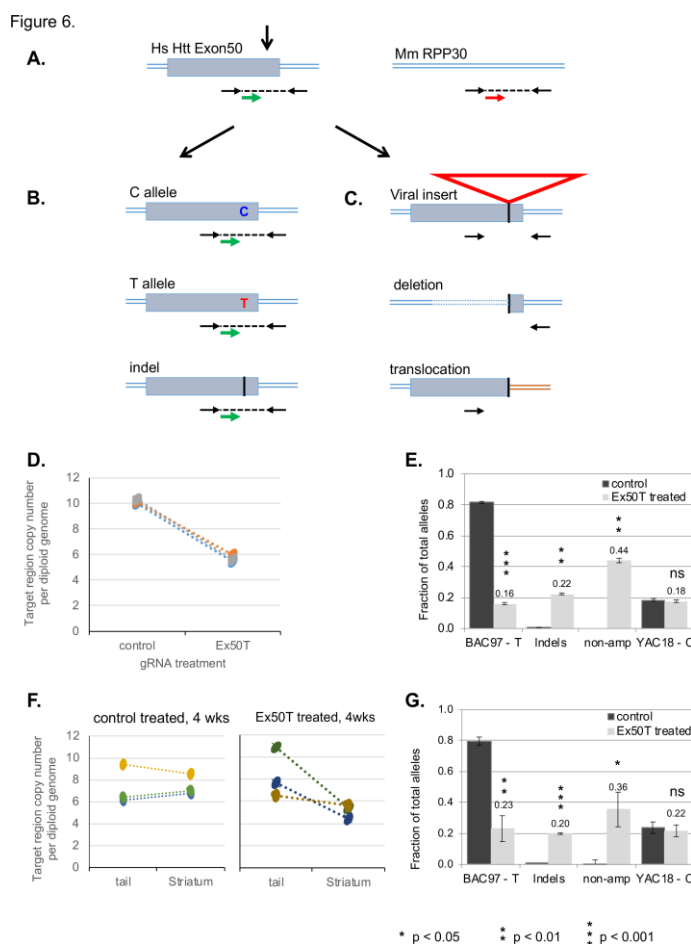


Figure 6. Analysis of non-amplified mutations by droplet digital PCR (ddPCR).

The relative copy number of human exon 50 was measured using primers (black arrows) and a probe (green arrow) flanking the CRISPR-Cas9 target site. A second set of primers and probe (red arrow) were used to determine the copy number of a reference locus, the mouse RPP30 gene. **B.** Following DNA cleavage and repair, ddPCR detects chromosomes with either of the original SNP allele sequences or small insertion/deletion (InDel) alleles. **C.** ddPCR does not detect chromosomes with mutations that either remove (large deletions) or separate (translations or large insertions) the primer binding sites. **D.** ddPCR was used to determine the total copy number of transgenic human HTT exon 50 in the primary neurons using the mouse RPP30 as a reference for the diploid genome. Samples were treated with lentivirus expressing Ex50T gRNA or a control (Rosa26) gRNA. Exon 50 copy number was decreased from an average of 10.2 to 5.7 across three paired neuronal samples. The 44% reduction reflects alleles that can no longer be amplified using

the primers for allele sequencing. **E.** The fraction of each allele class is estimated by multiplying the fraction of sequenced alleles by the estimated fraction of alleles that could be amplified (0.56) based on the ddPCR results. "non-amp" indicates the estimated fraction of alleles that could not be amplified. **F.** ddPCR was used to determine the total copy number of human HTT exon 50 in the four-week striatal samples treated with AAV expressing the Ex50T or a control (Rosa26) gRNA and in untreated tail DNA from the same animals. There was no significant difference in the exon 50 copy number between tails and striatum treated with the control gRNA. In contrast, the copy number was reduced by an average of 36% in striatum treated the the Ex50T gRNA. This reduction reflects alleles that can no longer be amplified using the primers for allele sequencing. **G.** The fraction of each allele class is estimated by multiplying the fraction of sequenced alleles by the estimated fraction of alleles that could be amplified (0.64) based on the ddPCR results. "non-amp" indicates the estimated fraction of alleles that could not be amplified. N=3 mice and error bars represent the S.E.M. p-values less than 0.05 were considered significant. Exact p-values are reported in Supplemental File 3.